Am J Transl Res 2020;12(7):3272-3287
www.ajtr.org /ISSN:1943-8141/AJTR0107781

Original Article

Protective effect of combined therapy with hyperbaric oxygen and autologous adipose-derived mesenchymal stem cells on renal function in rodent after acute ischemia-reperfusion injury

Sheung-Fat Ko[1], Kuan-Hung Chen[2], Christopher Glenn Wallace[3], Chih-Chao Yang[4], Pei-Hsun Sung[5], Pei-Lin Shao[6], Yi-Chen Li[5], Yen-Ta Chen[7], Hon-Kan Yip[5,6,8,9,10,11]

Departments of [1]Radiology, [2]Anesthesiology, Kaohsiung Chang Gung Memorial Hospital and Chang Gung University College of Medicine, Kaohsiung 83301, Taiwan; [3]Department of Plastic Surgery, University Hospital of South Manchester, Manchester, UK; [4]Division of Nephrology, [5]Division of Cardiology, Department of Internal Medicine, Kaohsiung Chang Gung Memorial Hospital and Chang Gung University College of Medicine, Kaohsiung 83301, Taiwan; [6]Department of Nursing, Asia University, Taichung 41354, Taiwan; [7]Division of Urology, Department of Surgery, Kaohsiung Chang Gung Memorial Hospital and Chang Gung University College of Medicine, Kaohsiung 83301, Taiwan; [8]Institute for Translational Research in Biomedicine, [9]Center for Shockwave Medicine and Tissue Engineering, Kaohsiung Chang Gung Memorial Hospital, Kaohsiung 83301, Taiwan; [10]Department of Medical Research, China Medical University Hospital, China Medical University, Taichung 40402, Taiwan; [11]Division of Cardiology, Department of Internal Medicine, Xiamen Chang Gung Hospital, Xiamen, Fujian, China

Received January 13, 2020; Accepted June 3, 2020; Epub July 15, 2020; Published July 30, 2020

Abstract: Background: This study tested the hypothesis that combined hyperbaric oxygen (HBO) and autologous adipose-derived mesenchymal stem cell (ADMSC) therapy was superior to either alone at protecting renal function in rodents after acute ischemia-reperfusion (IR) injury. Methods and results: Adult-male SD rats (n = 40) were equally categorized: group 1 (sham-operated control); group 2 (IR + 50 μg medium intra-renal artery administration); group 3 [IR + HBO (at 1.5 h and days 1 and 2 after IR)]; group 4 [IR + ADMSC (2.0×10^6 cells/5.0×10^5/per each renal artery and 1.0×10^6 by intravenous injection at 1.5 h after IR]; and group 5 (IR + HBO-ADMSC). By 72 hr after IR, the circulating levels of BUN/creatinine and ratio of urine protein/creatinine were significantly highest in group 2, lowest in group 1, significantly increased in group 5 than in groups 3 and 4, but not different between latter two groups, whereas the circulating levels of EPCs and soluble-angiogenesis biomarkers (SDF-1α/HIF-1α) exhibited an opposite pattern to BUN/creatinine among the five groups (all $P<0.001$). The kidney injury score, ROS (fluorescent intensity of H_2DCFDA dye in kidney), inflammation (F4/80+, CD14+ cells) and glomerular-tubular injury score (WT-1/KIM-1) displayed an identical pattern whereas the integrity of podocyte components exhibited an opposite pattern to BUN/creatinine among the five groups (all $P<0.0001$). The protein expressions of inflammatory (MMP-9/TNF-α/NF-κB/ICAM-1), oxidative-stress (NOX-1/NOx-2/oxidized protein) and apoptotic (mitochondrial-Bax/cleaved-caspase3/PARP) markers showed an identical pattern to BUN/creatinine (all $P<0.001$). Conclusion: Combined ADMSC-HBO therapy was superior to either one alone at protecting the kidney from acute IR injury.

Keywords: Ischemia-reperfusion, hyperbaric oxygen therapy, adipose-derived mesenchymal stem cell, inflammation, oxidative stress

Introduction

Acute kidney injury (AKI) is common and is defined as an acute loss of kidney function as measured by circulating creatinine level or estimated creatinine clearance rate [1]. AKI can be caused by various disease states, including postsurgical (such as following cardiopulmonary surgery or organ transplantation), hypoxia, hemodynamic instability and shock, toxic drugs and chemical compounds, mechanical trauma, inflammation, and obstructive uropathy [2-7]. Acute kidney ischemia-reperfusion (IR) injury is a major cause of AKI and shares causal etiolo-

gies that are independently predictive of increased mortality and care costs [2-4, 8-10]. Acute kidney IR injury is frequently associated with progression of chronic kidney disease (CKD) and renal replacement therapy is a last resort for treating its advanced stages. An effective and safe treatment for acute kidney IR injury/AKI is lacking and urgently sought.

The mechanisms involved in acute kidney IR injury/AKI have been extensively investigated and appear mainly to involve the generation of free radicals, oxidative stress, inflammation, mitochondrial damage and direct glomerular-tubular hypoxic/necrotic damage [11-16]. Plentiful data have shown that mesenchymal stem cells (MSCs) [12, 13, 15], especially adipose-derived MSCs (ADMSCs) [12, 13], have strong protective capacity for the kidney against acute kidney IR injury/AKI [12, 13, 15] via anti-inflammatory and immunomodulation [12, 13] effects. In addition, hyperbaric oxygen (HBO) has been utilized for poor wound healing in peripheral artery disease (PAD) patients [17-19] as it enhances oxygen delivery into ischemic tissues (i.e., hyperoxia), protecting the cells/tissues from hypoxia. Additionally, our recent study has shown that HBO therapy inhibited circulating level of inflammatory cytokine, augmented circulating levels of EPCs and angiogenesis factors, and improved the blood flow in the ischemic area [20]. Another our recent study has also demonstrated that HBO therapy protected against ischemia-reperfusion induced thigh injury mainly through suppressing inflammation, oxidative stress and DNA/mitochondrial damage, and enhancing angiogenesis [21]. Based on the aforementioned issues [11-21], this study tested the hypothesis that combined therapy with HBO and ADMSC would be superior to either one alone for protecting the kidney from acute IR injury.

Materials and methods

Ethics

All animal procedures were approved by the Institute of Animal Care and Use Committee at Kaohsiung Chang Gung Memorial Hospital (Affidavit of Approval of Animal Use Protocol No. 2017032802) and performed in accordance with the Guide for the Care and Use of Laboratory Animals.

Animals were housed in an Association for Assessment and Accreditation of Laboratory Animal Care International (AAALAC; Frederick, MD, USA)-approved animal facility in our hospital with controlled temperature and light cycles (24°C and 12/12 light cycle).

Animal model of acute kidney ischemia-reperfusion injury, animal grouping and treatment strategy

Pathogen-free, adult-male Sprague-Dawley (SD) rats (n = 40) weighing 325 g (Charles River Technology, BioLASCO Taiwan Co. Ltd., Taiwan) were equally divided into five groups (i.e., n = 10 for each group): Sham-operated control (SC) (laparotomy only); acute IR + intrarenal artery injection of 50 μL of ADMSC culture medium 1.5 h after IR procedure; IR + HBO ([i.e., intermittent HBO therapy at 1.5 h and at days 1 and 2 after the acute kidney IR procedure); IR + autologous ADMSC (5.0×10^5 cells/each kidney by left and right intrarenal artery injection, followed by 1.0×10^6 cells from tail vein administration at 1.5 h after IR procedure); and IR + HBO + autologous ADMSC.

The procedure and protocol of acute kidney IR were based on our previous reports [11, 14]. Animals in groups 1 to 5 were anesthetized by inhalational 2.0% isoflurane and placed supine on a warming pad at 37°C for midline laparotomies. SC animals underwent laparotomy only, while acute kidney IR of both kidneys was induced in all animals in groups 2 to 5 by clamping the renal pedicles for one hour using non-crushing vascular clips. The animals in each group were sacrificed and kidney specimens harvested for molecular-cellular study by day 3 after the acute kidney IR procedure. The dosage and time points of ADMSC administration to the animals were based on our recent reports [12, 13].

Identification of circulating creatinine and BUN levels, and collection of 24-hour urine for the ratio of urine protein to urine creatinine at baseline and 72 h after acute kidney IR

The procedure and protocol were based on our previous report [22] with some modifications. Blood samples were drawn from each animal to determine serum creatinine and blood urine nitrogen (BUN) levels at baseline and at 72 h after acute kidney IR procedure.

For the collection of 24-hr urine, each animal was put into a metabolic cage [DXL-D, space: 19×29×55 cm, Suzhou Fengshi Laboratory Animal Equipment Co. Ltd., Mainland China] for 24 h with free access to food and water and urine collected in all animals from 48 to 72 h after acute kidney IR procedure to determine daily the ratio of urine protein to urine creatinine.

Hyperbaric oxygen therapy

The procedure and protocol of hyperbaric oxygen (HBO) therapy was based on a previous report [17]. Briefly, to induce tissue-level hyperoxia, SD rats were subjected to HBO administration in an animal tabletop chamber (PiersolDive, model 4934) with the animals exposed to 100% oxygen at 2.4 atmospheres absolute (ATA) for 90 minutes (3 h/one time).

Procedure and protocol for isolating and culturing autologous ADMSCs

The procedure and protocol for autologous ADMSC isolation and culture have previously been described [12, 13, 23]. Briefly, adipose tissue surrounding the epididymis was dissected, excised and prepared by day 14 prior to acute kidney IR induction. For purification, the harvested cells were cultured in Dulbecco's modified Eagle's medium (DMEM)-low glucose medium containing 10% FBS for 14 days. By this time plentiful ADMSCs (i.e., approximately 2.5-3.0×10^6 cells) were obtained in the culture plate and were collected to treat AIS animals. Surface markers for ADMSCs were identified by flow cytometric analyses as previously reported [12, 13, 23]. The ADMSCs were stained by CellTracker™ Orange CMRA dye (Molecular probes) 30 minutes prior to administration to animals in groups 4 and 5.

Assessment of kidney injury scores at 72 after acute kidney IR procedure

The procedure and protocol were based on our previous reports [11, 12, 14]. Briefly, the harvested kidney specimens from all animals were fixed in 10% buffered formalin, embedded in paraffin, sectioned at 5 μm and stained with hematoxylin and eosin (H&E) for light microscopy. The scoring system reflected the grading of tubular necrosis, loss of brush border, cast formation, and tubular dilatation in 10 randomly chosen, non-overlapping fields (200×), as follows: 0 (none), 1 (≤10%), 2 (11-25%), 3 (26-45%), 4 (46-75%), and 5 (≥76%).

Immunohistochemical (IHC) and immunofluorescent (IF) staining

The procedure and protocols have been described by previous reports [11, 13, 14, 23]. Briefly, sections were incubated with primary antibodies specifically against zonula occludens-1 (ZO-1) (1:500, Novus), kidney injury molecule (KIM)-1 (1:500, R&D system), E-cadherin (1:200, Novus), snail (1:500, Abcam), fibronectin (1:200, Abcam), Wilms tumor (WT)-1 (1:200, Abcam), dystrophin (1:100, Abcam), nephrin (1:100, Bioss), CD31 (1:100, Bio-Rad), CD14 (1:200, Proteintech) and 4F/80 (1:100, Santa Cruz), while sections incubated with irrelevant antibodies served as controls. Three sections of kidney specimen from each rat were analyzed. For quantification, three random HPFs (400× for IHC and IF studies) were analyzed in each section. The mean number of positively-stained cells per HPF for each animal was then determined by summation of all numbers divided by 9.

An IHC-based/IF-based scoring system was adopted for semi-quantitative analyses of ZO-1, nephrin, CD31, dystroglycan, E-cadherin, KIM-1 and WT-1 in the kidneys as a percentage of positive cells in blinded fashion (score of positively-stained cell for these biomarkers as: 0 = negative staining; 1 = <15%; 2 = 15-25%; 3 = 25-50%; 4 = 50-75%; 5 = >75%-100%/per HPF).

Western blot analysis

Equal amounts (50 μg) of protein extracts were loaded and separated by SDS-PAGE using acrylamide gradients. After electrophoresis, the separated proteins were transferred electrophoretically to a polyvinylidene difluoride (PVDF) membrane (GE, UK). Nonspecific sites were blocked by incubation of the membrane in blocking buffer [5% nonfat dry milk in T-TBS (TBS containing 0.05% Tween 20)] overnight. The membranes were incubated with the indicated primary antibodies and β-actin (1:6000, Merck Millipore, Billerica, MA, USA) for 1 hour at room temperature. Horseradish peroxidase-conjugated anti-rabbit immunoglobulin IgG (1:2000, Cell Signaling, Danvers, MA, USA) was used as a secondary antibody for one-hour incubation at room temperature. The washing

procedure was repeated eight times within one hour. Immunoreactive bands were visualized by enhanced chemiluminescence (ECL; Amersham Biosciences, Amersham, UK) and exposed to Biomax L film (Kodak, Rochester, NY, USA). For quantification, ECL signals were digitized using Labwork software (UVP, Waltham, MA, USA). Uncropped, unedited blots were provided in Supplementary Figure 1.

Procedure and protocol for measurement of reactive oxygen species (ROS) in kidney parenchyma using H_2DCFDA dye by day 72 prior to sacrifice of animals

The procedure and protocol were based on our previous report [24]. To determine the fluorescent intensity of ROS in IR kidney, four additional animals were utilized in each study group. By the end of the study period (i.e., 30 min prior to sacrifice of the animal), rats were anesthetized with 2% isoflurane and 150 μg of CM-H_2DCFDA (Life Technologies Molecular Probes; 100 μg of H_2DCFDA was dissolved in 200 μl PBS) was slowly intravenously injected into each animal. The kidney was harvested 30 min after CM-H_2DCFDA injection, immediately frozen in liquid nitrogen, and cryostat sections (5 μm) were cut and placed in a cabinet maintained at -20°C. Serial frozen sections were fixed with 4% paraformaldehyde/phosphate buffered saline (PBS) at 4°C for 5 minutes. Sections were washed in PBS and then co-stained with DAPI for fluorescence microscopy analysis.

All sections were examined under a fluorescent microscope (200× magnification). Both captured fluorescence and gray photos were assessed by DP controller 2.1.1.183 (Olympus). Gray photos for measuring fluorescence intensity were processed by Image J 1.37v (National Institutes of Health, USA). Three gray photos from each section were randomly obtained, giving a total of nine photos for each animal. The fluorescent intensity was defined as score: 0 = unstaining; 1 = weak staining; 2 = moderate staining; and 3 = strong staining.

Statistical analysis

Quantitative data are expressed as means ± SD. Statistical analysis was adequately performed by ANOVA followed by Bonferroni multiple-comparison post hoc test. Statistical analysis was performed using SPSS statistical software for Windows version 22 (SPSS for Windows, version 22; SPSS, IL, U.S.A.). A value of $P<0.05$ was considered as statistically significant.

Results

*Population of MSCs after day-14 culturing and levels of BUN, creatinine, the ratio of urine protein to urine creatinine, and EPCs at baseline and by day 3 after IR procedure (**Figure 1**)*

CD29+ cell was the most popular MSC, followed by C73+ and CD90+ cells, respectively (**Figure 1A**). Additionally, by day 0, the circulating levels of BUN and creatinine did not differ among the five groups (**Figure 1C**, **1D**). However, by 72 h after IR procedure, these parameters were highest in IR, lowest in SC, significantly lower in IR-HBO-ADMSC than in IR-BHO and IR-ADMSC, and not different between the latter two groups (**Figure 1E**, **1F**). Moreover, by day 0, the ratio of urine protein to urine creatinine was similar among the five groups (**Figure 1G**). However, by 72 h after IR procedure, this parameter was significantly higher in IR than in other four groups, significantly higher in IR-HBO than in SC, IR-ADMSC and IR-HBO-ADMSC, but it showed no different among these later three groups (**Figure 1H**).

Prior to acute kidney IR induction, the circulating levels of KDR+/CD34+ and C-kit+/CD31+ cells, two EPC surface markers, did not differ among the five groups (**Figure 1I**, **1J**). However, the circulating level of Sca-1+/CD31+ cells, another circulating level of EPC surface marker, was significantly higher in SC, IR and IR-HBO than in IR-ADMSC and IR-HBO-ADMSC, but it showed no difference among the former three groups or between the later two groups (**Figure 1K**). Furthermore, the circulating level of VE-cadherin/CD34+ cells was significantly higher in SC, IR, IR-ADMSC than in IR-HBO-ADMSC but it showed no difference among the SC, IR, IR-HBO and IR-ADMSC, or between IR-HBO and IR-HBO-ADMSC (**Figure 1L**). By 72 h after IR procedure, these four circulating levels of EPC surface markers were significantly progressively increased from SC to IR-HBO-ADMSC group (**Figure 1M-P**).

*Fluorescent intensity of reactive oxygen species and kidney injury score by 72 h after IR procedure (**Figure 2**)*

IF microscopy demonstrated that the fluorescent intensity of H_2DCFDA dye staining in kid-

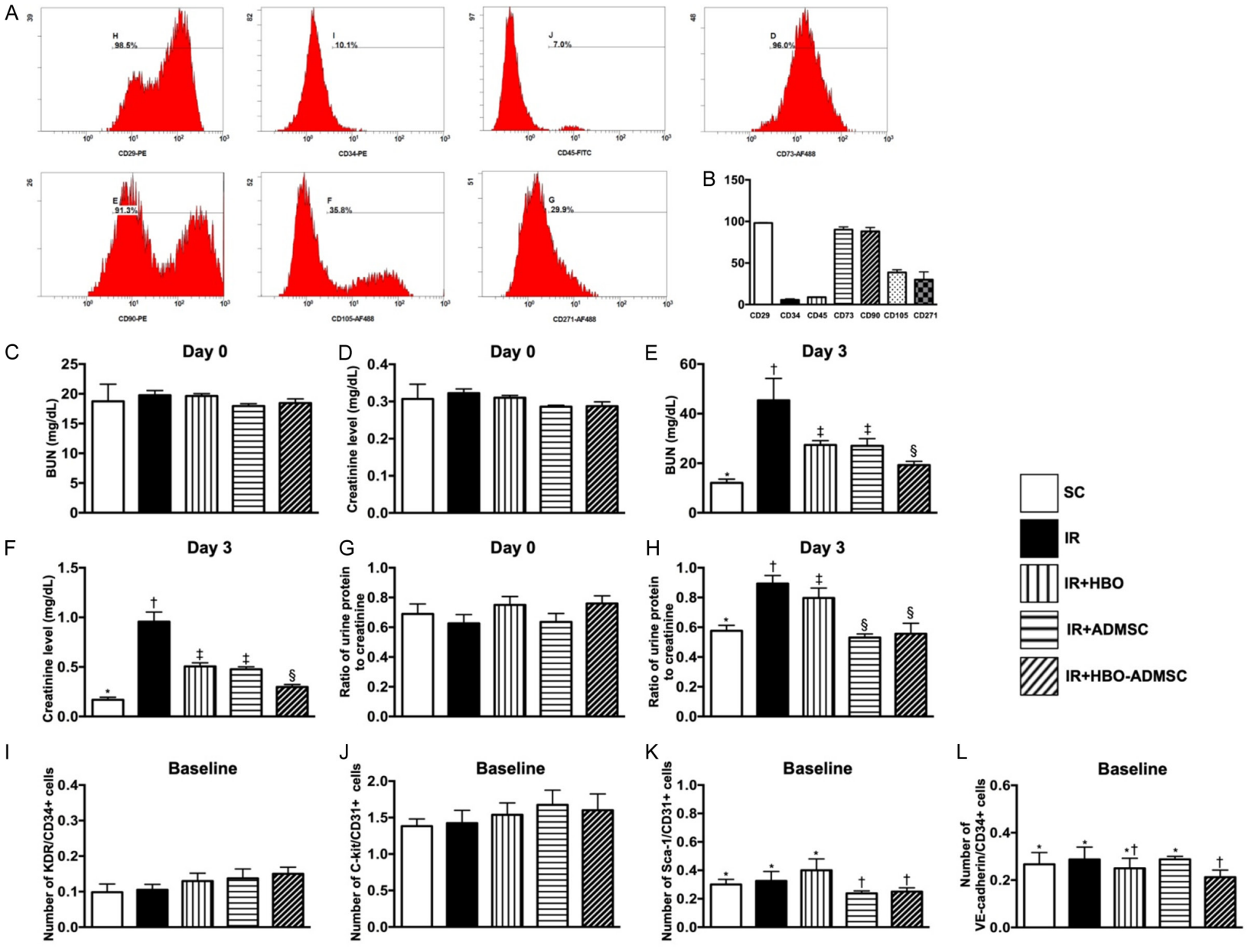
A
H
98.5%
CD29-PE
I
10.1%
CD34-PE
J
7.0%
CD45-FITC
D
96.0%
CD73-AF488
E
91.3%
CD90-PE
F
35.8%
CD105-AF488
G
29.9%
CD271-AF488
B
CD29
CD34
CD45
CD73
CD90
CD105
CD271
C
Day 0
BUN (mg/dL)
D
Day 0
Creatinine level (mg/dL)
E
Day 3
BUN (mg/dL)
F
Day 3
Creatinine level (mg/dL)
G
Day 0
Ratio of urine protein to creatinine
H
Day 3
Ratio of urine protein to creatinine
SC
IR
IR+HBO
IR+ADMSC
IR+HBO-ADMSC
I
Baseline
Number of KDR/CD34+ cells
J
Baseline
Number of C-kit/CD31+ cells
K
Baseline
Number of Sca-1/CD31+ cells
L
Baseline
Number of VE-cadherin/CD34+ cells

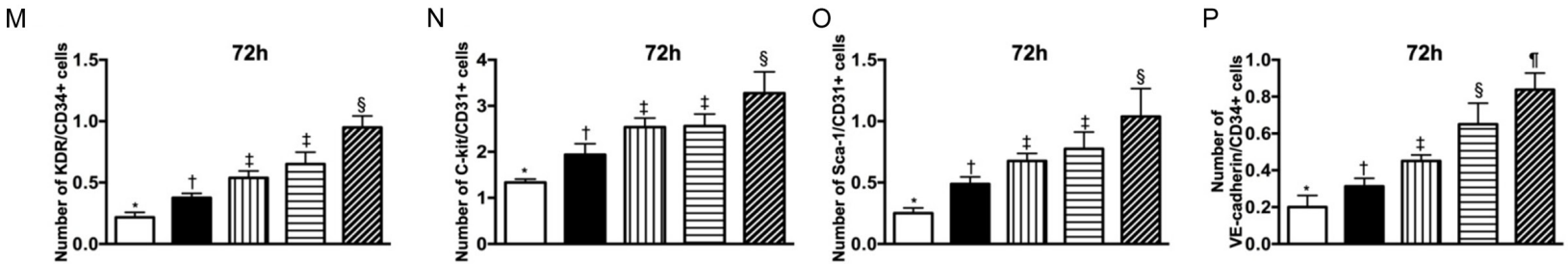

Figure 1. Distribution of mesenchymal stem cells (MSC) after day-14 cell culture, levels of BUN, creatinine and the ratio of urine protein to urine creatinine, and circulating EPCs at baseline and by 72 h after kidney IR injury. A. Illustrating the results of flow cytometric analysis of MSCs by day 14 after cell culturing. B. Analytic result of percentage of MSC distribution. C. By day 0, circulating level of blood urine nitrogen (BUN), P>0.5. D. By day 0, circulating level of creatinine, P>0.5. E. By day 3 after IR procedure, the circulating level of BUN, * vs. other groups with different symbols (†, ‡, §, ¶), P<0.0001. F. By day 3 after IR procedure, circulating level of creatinine, * vs. other groups with different symbols (†, ‡, §, ¶), P<0.0001. G. By day 0, the ratio of urine protein to urine creatinine, P>0.5. H. By day 3 after IR procedure, the ratio of urine protein to urine creatinine, * vs. other groups with different symbols (†, ‡), P<0.001. I. At baseline, number of circulating KDR+/CD34+ cells, P>0.5. J. At baseline, number of circulating C-kit+/CD31+ cells, P>0.5. K. At baseline, number of circulating Sca-1+/CD31+ cells, * vs. †, P<0.04. L. At baseline, number of circulating VE-cadherin+/CD34+ cells, * vs. †, P<0.05. M. By 72 h after IR procedure, number of circulating KDR+/CD34+ cells, * vs. other groups with different symbols (†, ‡, §), p<0.0001. N. By 72 h, number of circulating C-kit+/CD31+ cells, * vs. other groups with different symbols (†, ‡, §), p<0.0001. O. By 72 h, number of circulating Sca-1+/CD31+ cells, * vs. other groups with different symbols (†, ‡, §), p<0.0001. P. By 72 h, number of circulating VE-cadherin+/CD34+ cells, * vs. other groups with different symbols (†, ‡, §, ¶), P<0.0001. All statistical analyses were performed by one-way ANOVA, followed by Bonferroni multiple comparison post hoc test (n = 6 for each group). Symbols (*, †, ‡, §, ¶) indicate significance (at 0.05 level). EPCs = endothelial progenitor cells (EPCs; SC = sham-operated control; IR = ischemia reperfusion; HBO = hyperbaric oxygen therapy; ADMSC = adipose-derived mesenchymal stem cell.

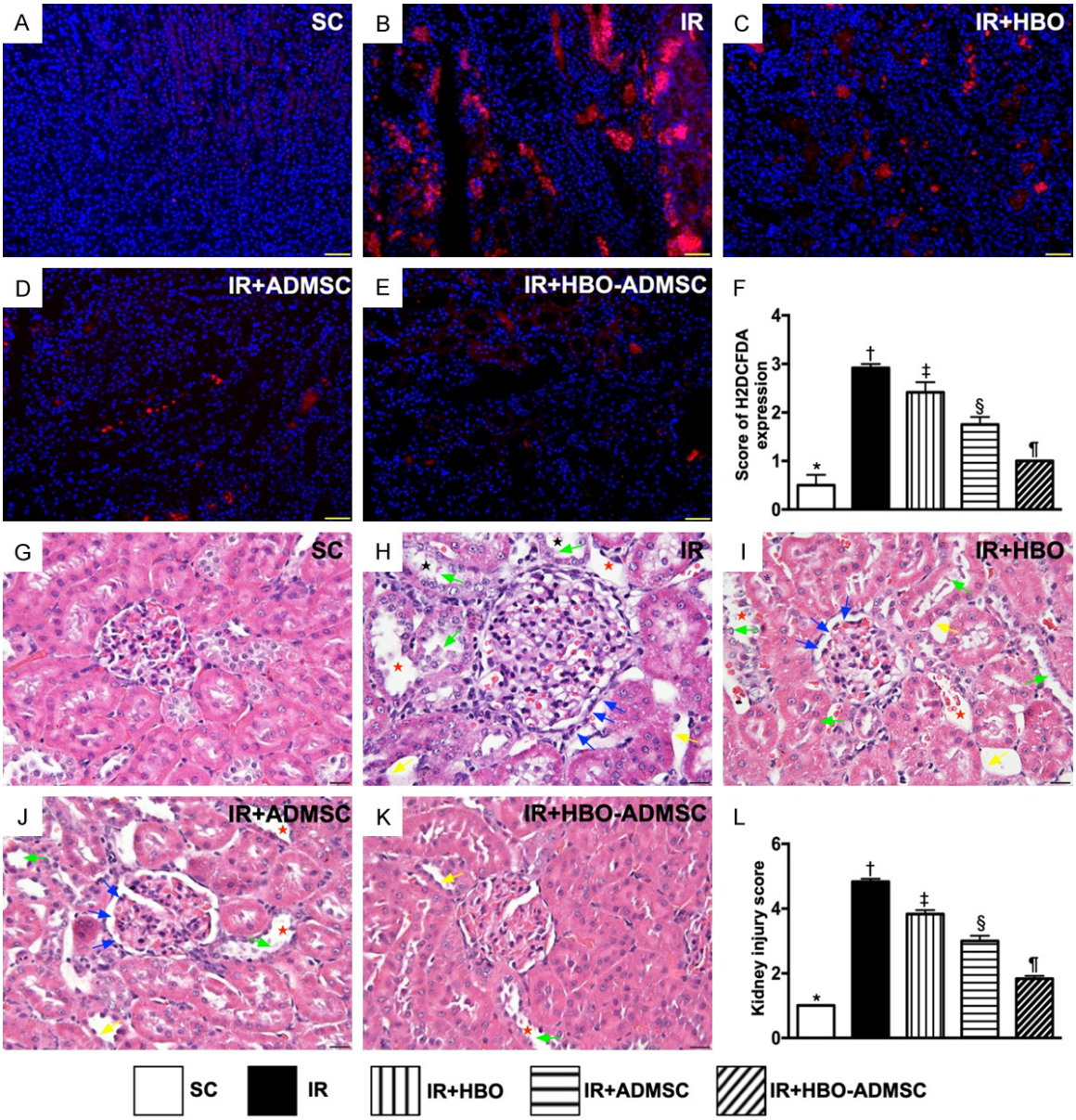

Figure 2. Fluorescent intensity of reactive oxygen species and histopathological findings of kidney injury score by 72 h after IR procedure. A-E. Immunofluorescent microscopic finding (400×) for identification of fluorescent intensity of oxidative stress (i.e., H_2DCFDA dye staining in kidney parenchyma) (red color). F. Analytical result of fluorescent intensity of oxidative stress, * vs. other groups with different symbols (†, ‡, §, ¶), P<0.0001. G-K. Light microscopic findings of H. & E. stain (400×) demonstrating significantly higher degree of loss of brush border in renal tubules (yellow arrows), tubular necrosis (green arrows), tubular dilatation (red asterisk) protein cast formation (black asterisk), and dilatation of Bowman's capsule (blue arrows) in IR group than in other groups. L. * vs. other groups with different symbols (†, ‡, §, ¶), P<0.0001. Scale bars in right lower corner represent 20 μm. All statistical analyses were performed by one-way ANOVA, followed by Bonferroni multiple comparison post hoc test (n = 6 for each group). All statistical analyses were performed by one-way ANOVA, followed by Bonferroni multiple comparison post hoc test (n = 4 for each group). Symbols (*, †, ‡, §, ¶) indicate significance (at 0.05 level). SC = sham-operated control; IR = ischemia reperfusion; HBO = hyperbaric oxygen therapy; ADMSC = adipose-derived mesenchymal stem cell.

ney parenchyma, an indicator of ROS, was highest in IR, lowest in SC, significantly lower in IR-HBO-ADMS than in IR-HBO and IR-ADMSC, and significantly lower in IR-ADMSC than in IR-HBO (**Figure 2A-F**). Additionally, H.E. staining showed that the kidney injury score displayed an identical pattern to ROS among the five groups (**Figure 2G-L**).

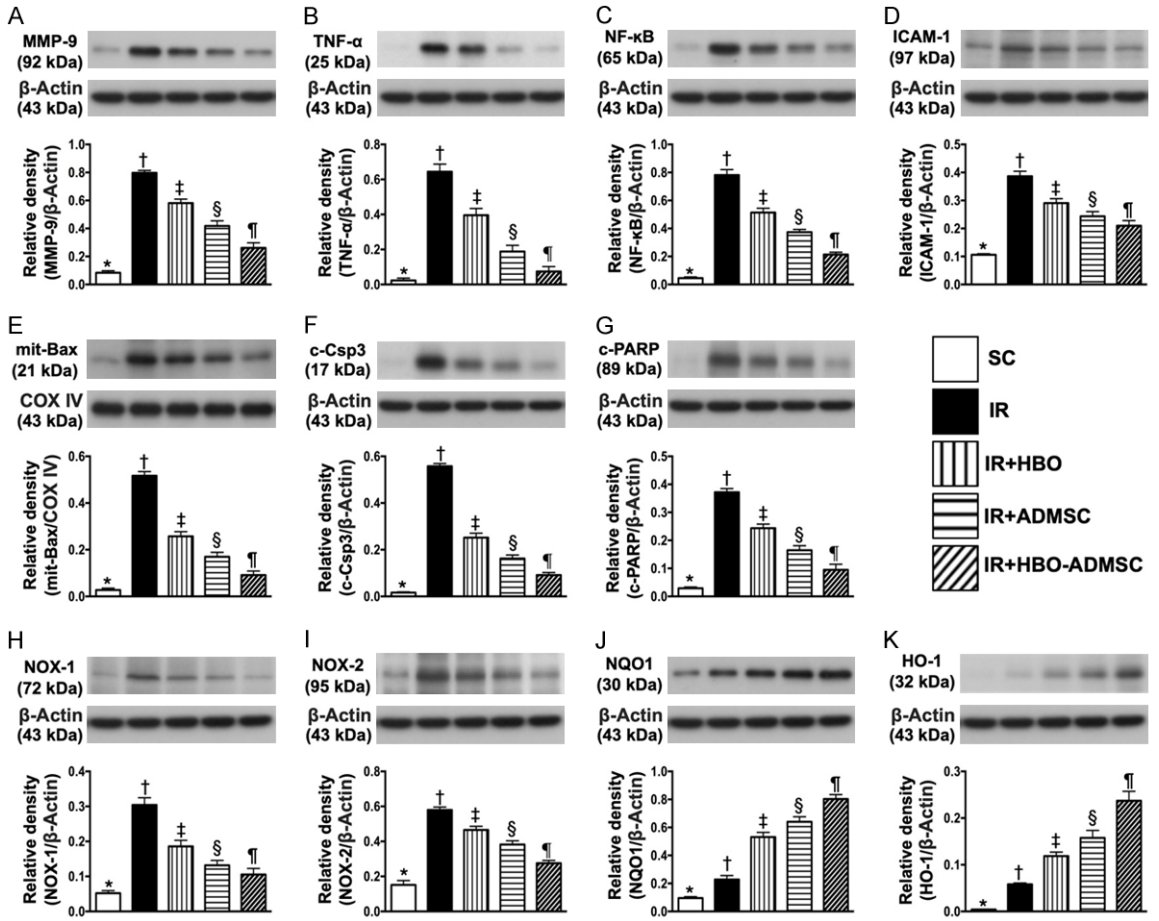

Figure 3. Protein expressions of inflammation, apoptosis, oxidative stress and anti-oxidant by 72 h after IR procedure. A. Protein expression of matrix metalloproteinase (MMP)-9, * vs. other groups with different symbols (†, ‡, §, ¶), P<0.0001. B. Protein expression of tumor necrotic factor (TNF)-α, * vs. other groups with different symbols (†, ‡, §, ¶), P<0.0001. C. Protein expression of nuclear factor (NF)-κB, * vs. other groups with different symbols (†, ‡, §, ¶), P<0.0001. D. Protein expression of intercellular adhesion molecule (ICAM)-1, * vs. other groups with different symbols (†, ‡, §, ¶), P<0.0001. E. Protein expression of mitochondrial (mito)-Bax, * vs. other groups with different symbols (†, ‡, §, ¶), P<0.0001. F. Protein expression of cleaved caspase 3 (c-Casp 3), * vs. other groups with different symbols (†, ‡, §, ¶), P<0.0001. G. Protein expression of cleaved poly ADP ribose polymerase (c-PARP), * vs. other groups with different symbols (†, ‡, §, ¶), P<0.0001. H. Protein expression of NOX-1, * vs. other groups with different symbols (†, ‡, §, ¶), P<0.0001. I. Protein expression of NOX-2, * vs. other groups with different symbols (†, ‡, §, ¶), P<0.0001. J. Protein expression of NAD(P)H quinone dehydrogenase (NQO) 1, * vs. other groups with different symbols (†, ‡, §, ¶), P<0.0001. K. Protein expression of heme oxygenase (HO)-1, * vs. other groups with different symbols (†, ‡, §, ¶), P<0.0001. All statistical analyses were performed by one-way ANOVA, followed by Bonferroni multiple comparison post hoc test (n = 6 for each group). Symbols (*, †, ‡, §, ¶) indicate significance (at 0.05 level). SC = sham-operated control; IR = ischemia reperfusion; HBO = hyperbaric oxygen therapy; ADMSC = adipose-derived mesenchymal stem cell.

*The protein expressions of inflammation, apoptosis, oxidative stress and anti-oxidant by 72 h after IR procedure (**Figure 3**)*

The protein expressions of MMP-9, TNF-α, NF-κB and ICAM-1, four indices of inflammation, were highest in IR, lowest in SC, significantly lower in IR-HBO-ADMSC than in IR-HBO and IR-ADMSC, and significantly lower in IR-ADMSC than in IR-HBO (**Figure 3A-D**). Additionally, the protein expressions of mitochondrial Bax, cleaved caspase 3 and cleaved PARP, three indicators of apoptosis, exhibited an identical pattern to inflammation among the five groups (**Figure 3E**, **3G**).

The protein expressions of NOX-1 and NOX-2, two indicators of oxidative stress, were highest in IR, lowest in SC, significantly lower in IR-HBO-ADMSC than in IR-HBO and IR-ADMSC, and significantly lower in IR-ADMSC than in IR-HBO (**Figure 3H**, **3I**). Conversely, the protein expres-

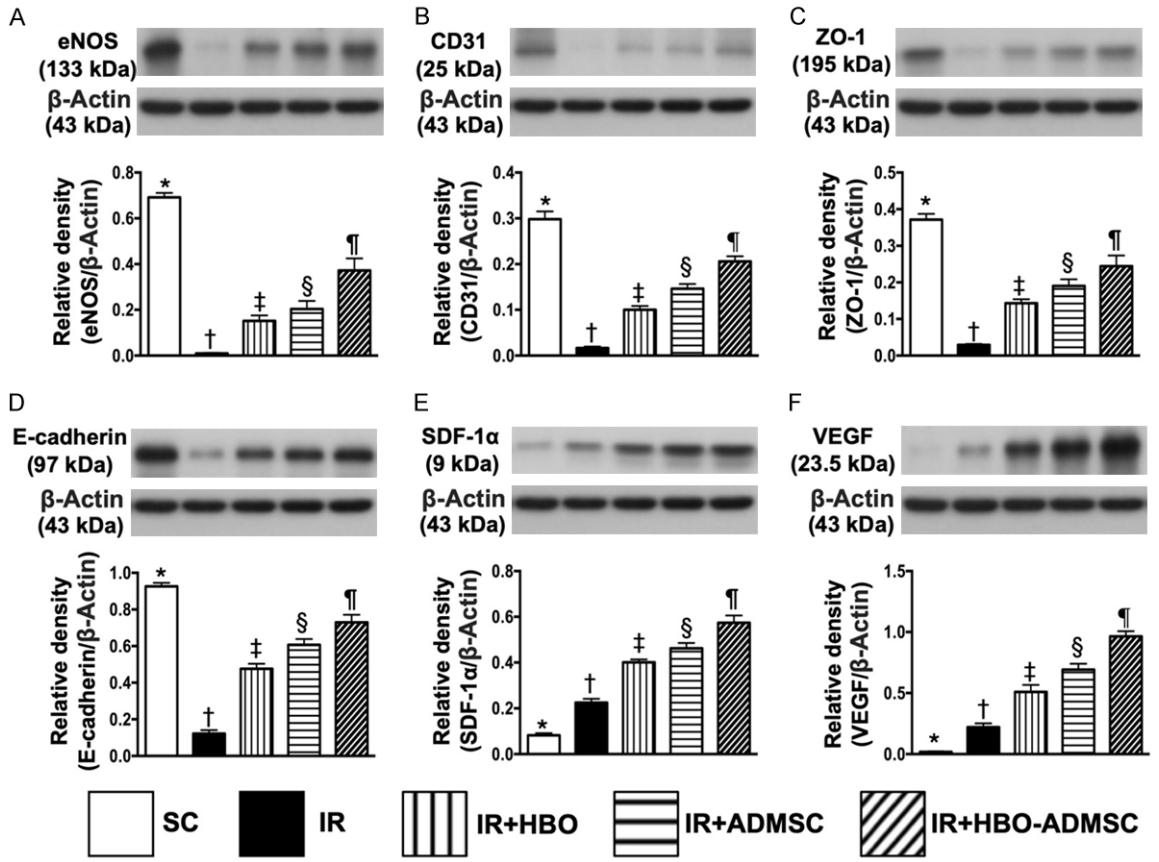

Figure 4. Protein expressions of angiogenesis factors and integrity of podocyte components by 72 h after IR procedure. A. Protein expression of endothelial nitric oxide synthase (eNOS), * vs. other groups with different symbols (†, ‡, §, ¶), P<0.0001. B. Protein expression of CD13, * vs. other groups with different symbols (†, ‡, §, ¶), P<0.0001. C. Protein expression of ZO-1, * vs. other groups with different symbols (†, ‡, §, ¶), P<0.0001. D. Protein expression of E-cadherin, * vs. other groups with different symbols (†, ‡, §, ¶), P<0.0001. E. Protein expression of stromal cell-derived factor (SDF)-1α, * vs. other groups with different symbols (†, ‡, §, ¶), P<0.0001. F. Protein expression of vascular endothelial growth factor (VEGF), * vs. other groups with different symbols (†, ‡, §, ¶), P<0.0001. All statistical analyses were performed by one-way ANOVA, followed by Bonferroni multiple comparison post hoc test (n = 6 for each group). Symbols (*, †, ‡, §, ¶) indicate significance (at 0.05 level). SC = sham-operated control; IR = ischemia reperfusion; HBO = hyperbaric oxygen therapy; ADMSC = adipose-derived mesenchymal stem cell.

sions of NQO 1 and HO-1, two indicators of antioxidants, displayed an opposite pattern to oxidative stress among the five groups (**Figure 3J**, **3K**).

*Protein expressions of angiogenesis factors and integrity of podocyte components by 72 h after IR procedure (**Figure 4**)*

Protein expression of eNOS and CD31, two indicators of endothelial cell integrity were highest in SC, lowest in IR, significantly higher in IR-HBO-ADMSC than in IR-HBO and IR-ADMSC, and significantly higher in IR-ADMSC than in IR-HBO (**Figure 4A**, **4B**). Additionally, the protein expressions of ZO-1 and E-cadherin, two indicators of podocyte integrity, exhibited an identical pattern to CD31 among the five groups (**Figure 4C**, **4D**). Furthermore, the protein expressions of SDF-1α and VEGF, two indicators of angiogenesis, progressively increased from SC to IR-HBO-ADMSC (**Figure 4E**, **4F**), highlighting an intrinsic response to IR stimulation that was further enhanced by HBO-ADMSC therapy.

*Cellular expressions of inflammation in kidney parenchyma by 72 h after IR procedure (**Figure 5**)*

IF microscopy showed that the positively-stained cell makers of F4/80 (**Figure 5A-F**) and CD14 (**Figure 5G-L**), two indicators of inflammation, were highest in IR, lowest in SC, significantly lower in IR-HBO-ADMSC than in IR-HBO and IR-ADMSC, and significantly lower in IR-ADMSC than IR-HBO.

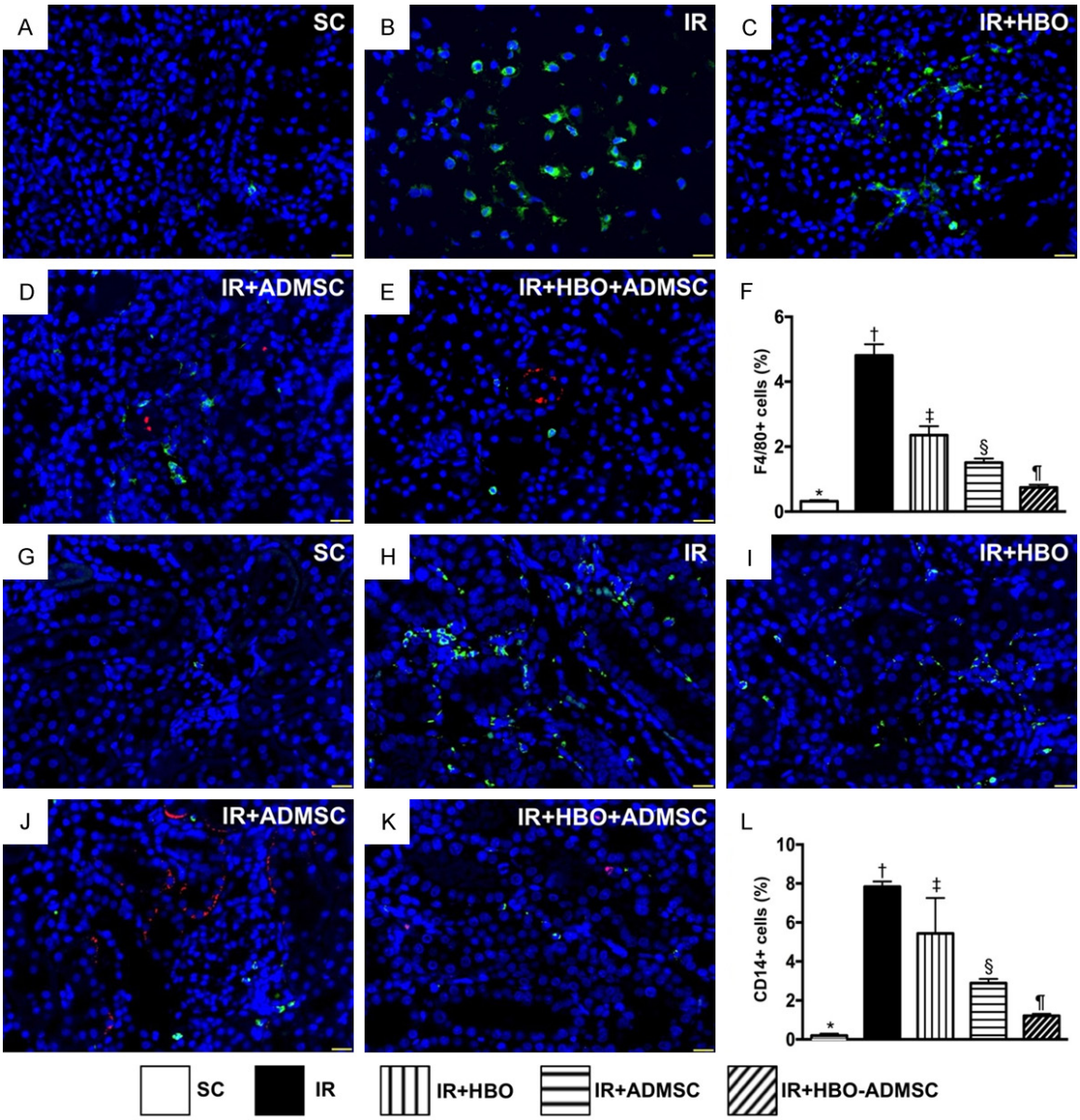

Figure 5. Cellular expressions of inflammation in kidney parenchyma by 72 h after IR procedure. (A-E) Illustrating immunofluorescent (IF) microscopic finding (400×) for identification of F4/80+ cells (green color). (F) Analytical result of number of F4/80+ cells, * vs. other groups with different symbols (†, ‡, §, ¶), P<0.0001. The red color with DAPI stained nucleus in (D) and (E) indicated the dye-labeling ADMSCs. (G-K) Showing the IF microscopic finding (400×) for identification of CD14+ cells (green color). (L) Analytical result of number of CD14+ cells, * vs. other groups with different symbols (†, ‡, §, ¶), P<0.0001. The red color with DAPI stained nucleus in (J) and (K) indicated the dye-labeling ADMSCs. Scale bars in lower right corner represent 20 μm. All statistical analyses were performed by one-way ANOVA, followed by Bonferroni multiple comparison post hoc test (n = 6 for each group). Symbols (*, †, ‡, §, ¶) indicate significance (at 0.05 level). SC = sham-operated control; IR = ischemia reperfusion; HBO = hyperbaric oxygen therapy; ADMSC = adipose-derived mesenchymal stem cell.

*The cellular expression of integrity of endothelial cell in kidney parenchyma and renal glomerulus component of fibronectin by 72 h after IR procedure (**Figure 6**)*

IF microscopy demonstrated that the cellular expression of CD31, an indicator of endothelial cell integrity, was highest in SC, lowest in IR, significantly higher in IR-HBO-ADMSC than in IR-HBO and IR-ADMSC, and significantly higher in IR-ADMSC than in IR-BHO (**Figure 6A-F**). IF microscopy showed that fibronectin, predominantly in the renal glomerulus, exhibited an identical pattern to endothelial cells among the five groups (**Figure 6G-L**).

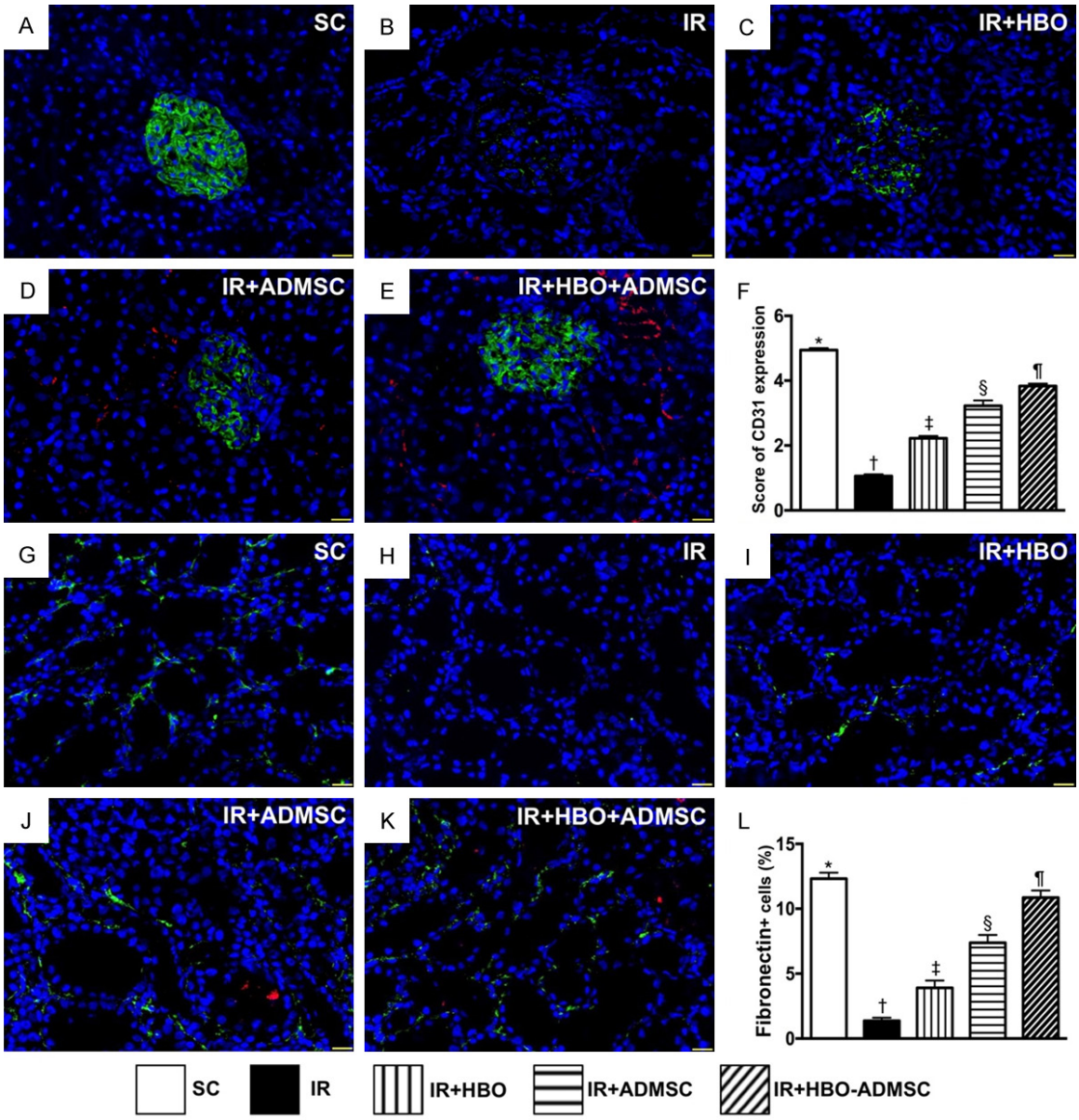

Figure 6. The cellular expression of integrity of endothelial cell in kidney parenchyma and renal glomerulus component of fibronectin by 72 h after IR procedure. (A-E) Showing the immunofluorescent (IF) finding (400×) for identification of cellular expression of CD31 (green color). (F) Analytical result of positively stained CD31 expression, * vs. other groups with different symbols (†, ‡, §, ¶), P<0.0001. The red color with DAPI stained nucleus in (D) and (E) indicated the dye-labeling ADMSCs. (G-K) Illustrating the IF microscopic finding (400×) for identification of fibronectin predominantly in the renal glomerulus (green color). (L) Analytical results of fibronectin expression, * vs. other groups with different symbols (†, ‡, §, ¶), P<0.0001. The red color with DAPI stained nucleus in (J) and (K) indicated the dye-labeling ADMSCs. Scale bars in lower right corner represent 20 μm. All statistical analyses were performed by one-way ANOVA, followed by Bonferroni multiple comparison post hoc test (n = 6 for each group). Symbols (*, †, ‡, §, ¶) indicate significance (at 0.05 level). SC = sham-operated control; IR = ischemia reperfusion; HBO = hyperbaric oxygen therapy; ADMSC = adipose-derived mesenchymal stem cell.

*Expressions of podocyte and renal tubular components by 72 h after IR procedure (**Figures 7** and **8**)*

The expressions of ZO-1 (**Figure 7A-F**) and dystrophin (**Figure 7G-L**) in glomeruli, two integrity of podocyte components, were highest in SC, lowest in IR, significantly higher in IR-HBO-ADMSC than in IR-HBO and IR-ADMSC, and significantly higher in IR-ADMSC than in IR-HBO. Additionally, the expression of nephrin **Figure 8A-F**), another indicator of podocyte component integrity in glomeruli, whereas the expression of E-cadherin (**Figure 8G-L**), predominantly

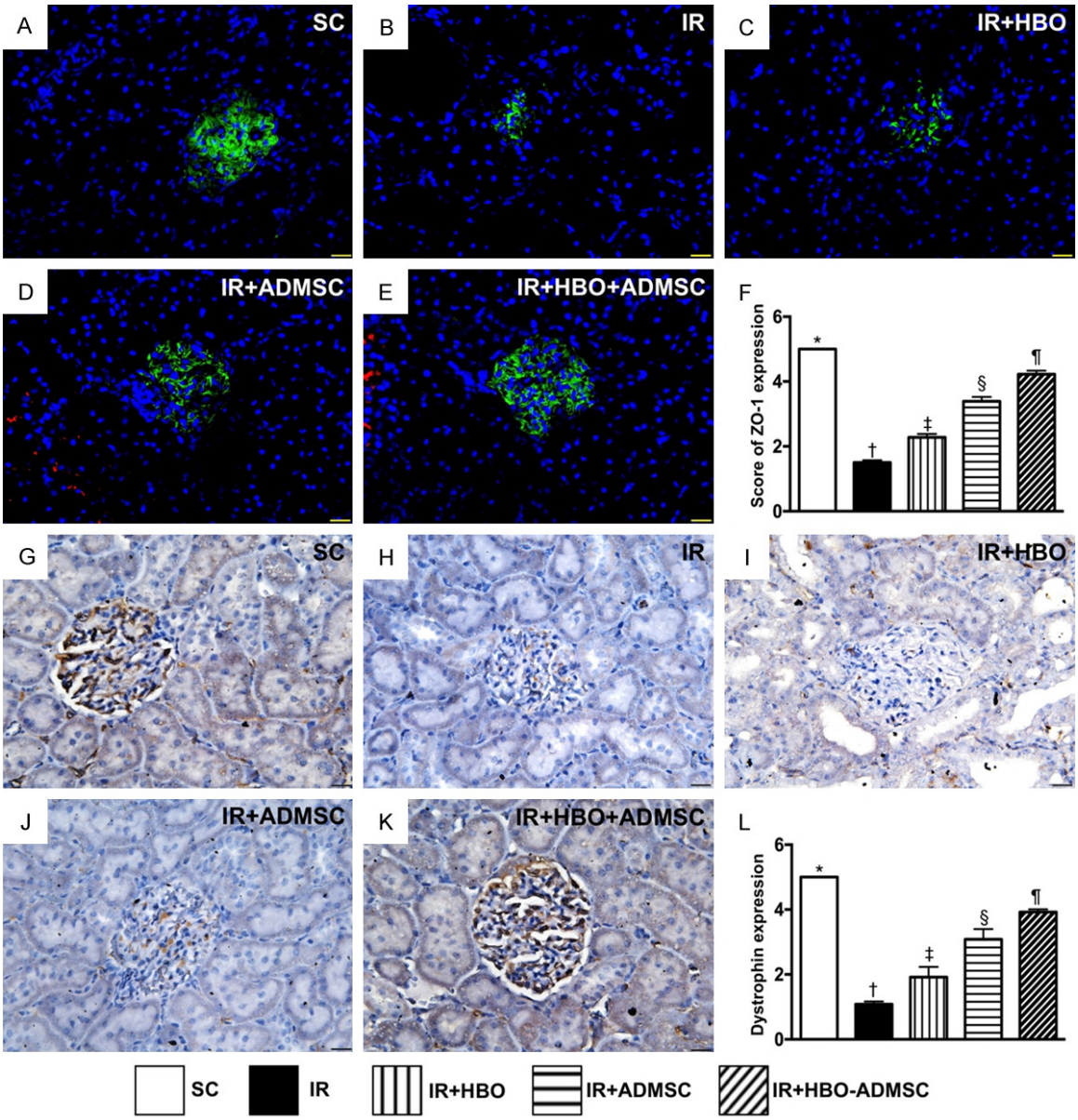

Figure 7. Expressions of podocyte components of ZO-1 and dystrophin by 72 h after IR procedure. (A-E) Illustrating immunofluorescent microscopic finding (400×) for identification of ZO-1 expression (green color). (F) Analytical result of ZO-1 expression, * vs. other groups with different symbols (†, ‡, §, ¶), P<0.0001. The red color with DAPI stained nucleus in (D) and (E) indicated the dye-labeling ADMSCs. (G-K) Illustrating immunohistochemical staining finding (400×) for identification of dystrophin expression (gray color). (L) Analytical result of dystrophin expression, * vs. other groups with different symbols (†, ‡, §, ¶), P<0.0001. Scale bars in lower right corner represent 20 μm. All statistical analyses were performed by one-way ANOVA, followed by Bonferroni multiple comparison post hoc test (n = 6 for each group). Symbols (*, †, ‡, §, ¶) indicate significance (at 0.05 level). SC = sham-operated control; IR = ischemia reperfusion; HBO = hyperbaric oxygen therapy; ADMSC = adipose-derived mesenchymal stem cell.

in renal tubule, displayed an identical pattern to ZO-1 among the five groups.

*The cellular expressions of Wilm's tumor suppressor gene 1 (WT-1) and KIM-1 by 72 h after IR procedure (**Figure 9**)*

IHC microscopic finding demonstrated that the cellular expression of WT-1, predominantly in podocytes, was highest in IR, lowest in SC, significantly lower in IR-HBO-ADMSC than in IR-ADMSC and IR-HBO, and significantly lower in IR-ADMSC than in IR-HBO **Figure 9A-F**). IF microscopic analysis consistently demonstrated that change in KIM-1, a kidney injury biomarker predominantly expressed in renal tubules, displayed an identical pattern to that of WT-1 among the five groups **Figure 9G-L**).

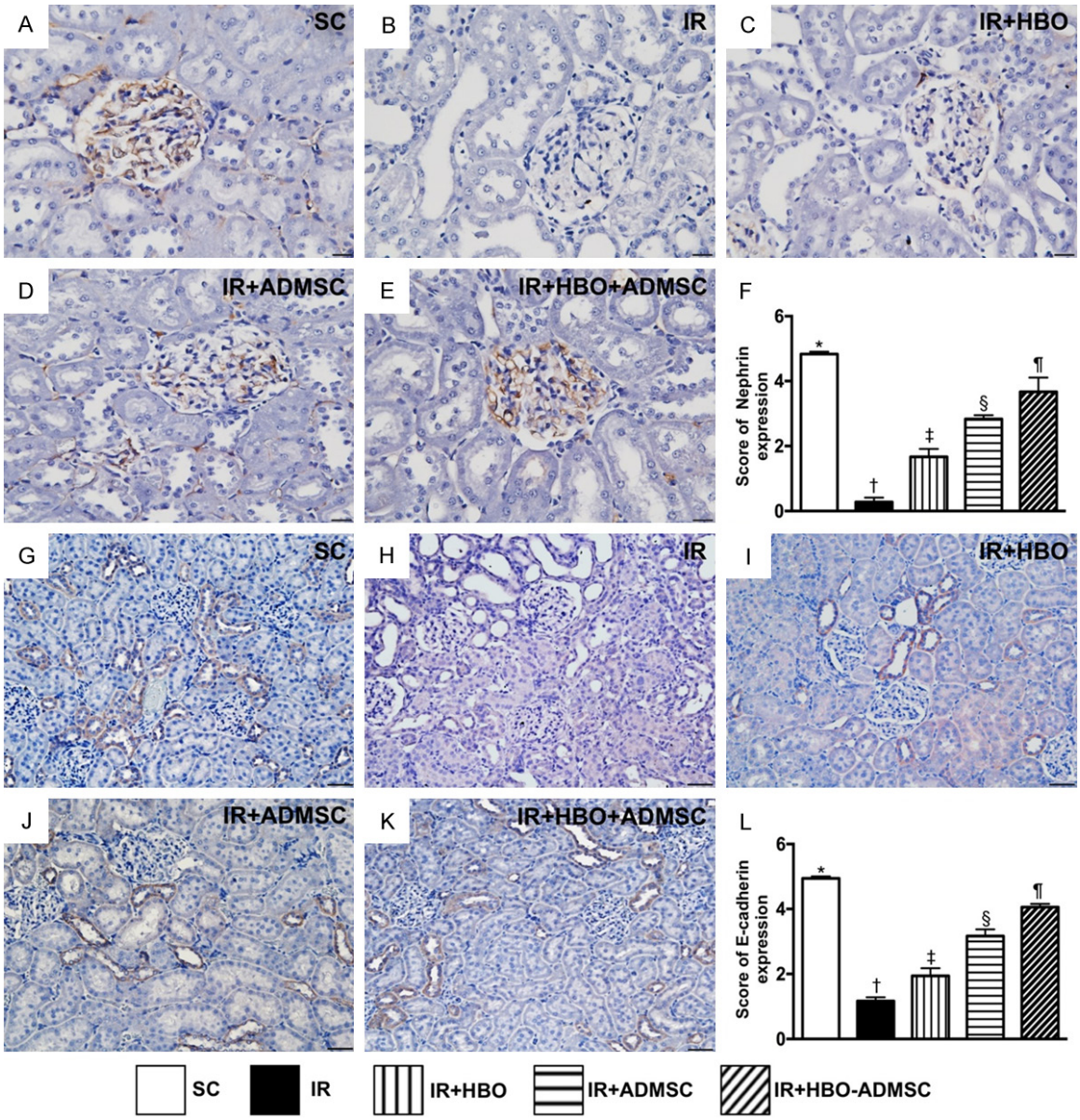

Figure 8. Expressions of nephrin in glomeruli and E-cadherin in renal tubule by 72 h after IR procedure. A-E. Showing immunohistochemical (IHC) staining (400×) for identification of the expression of nephrin in glomeruli (gray color). F. Analytic result of the expression of nephrin, * vs. other groups with different symbols (†, ‡, §, ¶), P<0.0001. G-K. IHC staining (400×) for identification of E-cadherin in renal tubule (gray color). L. Analytical result of E-cadherin expression, * vs. other groups with different symbols (†, ‡, §, ¶), P<0.0001. Scale bars in lower right corner represent 20 μm. All statistical analyses were performed by one-way ANOVA, followed by Bonferroni multiple comparison post hoc test (n = 6 for each group). Symbols (*, †, ‡, §, ¶) indicate significance (at 0.05 level). SC = sham-operated control; IR = ischemia reperfusion; HBO = hyperbaric oxygen therapy; ADMSC = adipose-derived mesenchymal stem cell.

Discussion

The most important finding in the present study was that, compared with SC, renal function (i.e., creatinine, BUN and proteinuria parameters) was significantly impaired in IR animals and significantly reversed by HBO or AMDSC therapy, and yet further significantly reversed by combined HBO-ADMSC therapy. To the best of our knowledge, this is the first report of this innovative treatment modality in the literature. Our results are attractive and promising, highlighting that this therapeutic regimen could be promptly translated into clinical application for patients who have severe AKI and are refractory to conventional therapy.

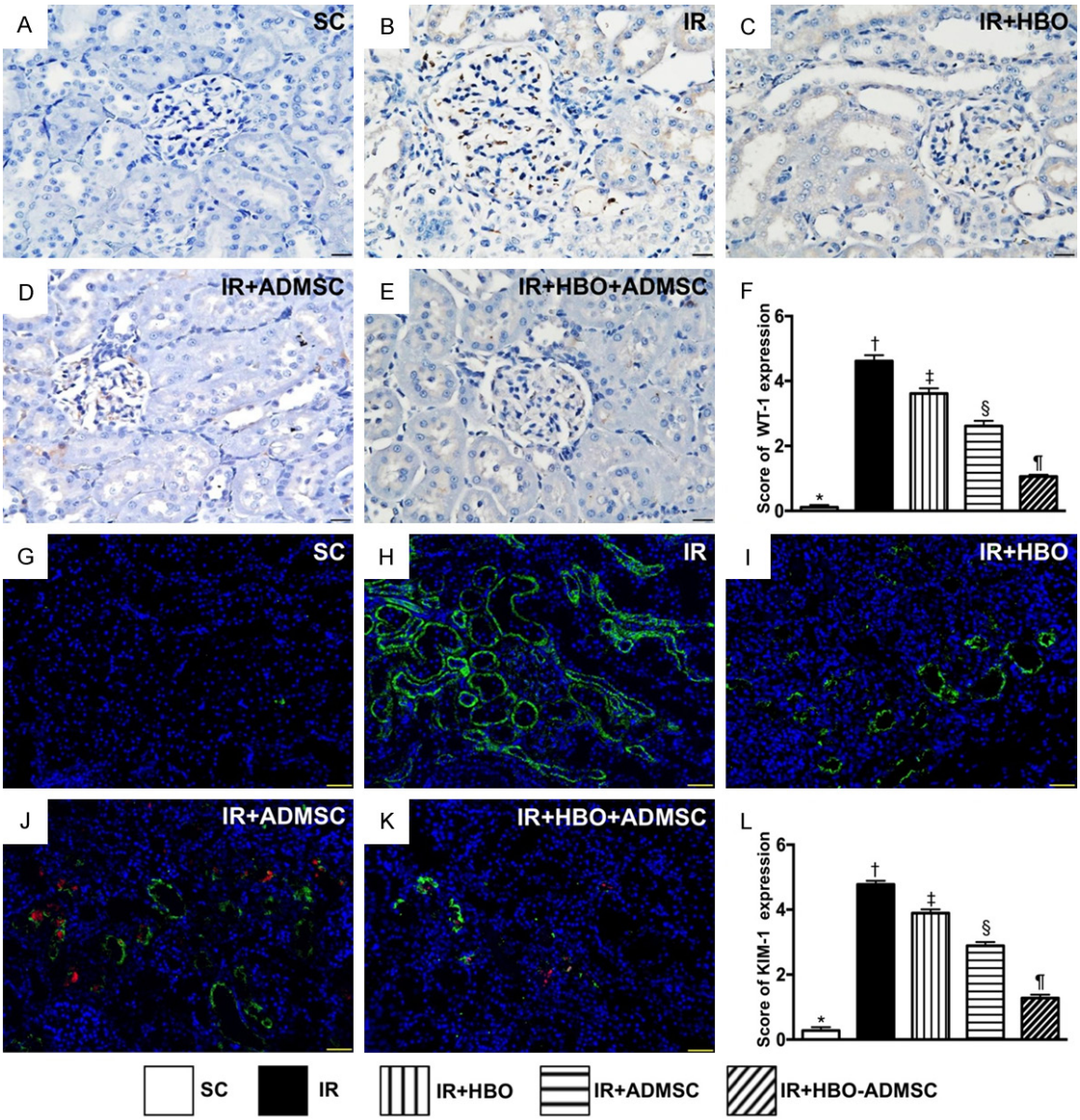

Figure 9. Cellular expressions of Wilm's tumor suppressor gene 1 (WT-1) and kidney injury molecule (KIM)-1 by 72 h after IR procedure. (A-E) Immunohistochemical staining (400×) for identification of the expression of WT-1 in glomeruli (gray). (F) Analytic result of the expression of WT-1, * vs. other groups with different symbols (†, ‡, §, ¶), P<0.0001. (G-K) Immunofluorescent microscopic finding (400×) for identification of KIM-1 in renal tubules (green color). (L) Analytical result of KIM-1 expression, * vs. other groups with different symbols (†, ‡, §, ¶), P<0.0001. The red color with DAPI stained nucleus in (J) and (K) indicated the dye-labeling ADMSCs. Scale bars in lower right corner represent 20 μm. All statistical analyses were performed by one-way ANOVA, followed by Bonferroni multiple comparison post hoc test (n = 6 for each group). Symbols (*, †, ‡, §, ¶) indicate significance (at 0.05 level). SC = sham-operated control; IR = ischemia reperfusion; HBO = hyperbaric oxygen therapy; ADMSC = adipose-derived mesenchymal stem cell.

It is well known that inflammatory reaction and oxidative stress will always be elevated in tissues/organs in acute ischemic or IR situations [11-14, 16, 23]. These situations, in turn, will damage mitochondria and generate more oxidative stress, free radicals and overwhelming inflammation, creating a vicious cycle of tissue/organ damage that leads to cellular apoptosis and death [11-14, 16, 23]. An essential finding in the present study was that oxidative stress and inflammation were remarkably increased IR animals than SC animals. Our findings were

consistent with those of previous studies [11-14, 16, 23], and could partially explain why the proteinuria, creatinine and BUN levels (i.e., indices of deteriorating renal function), and kidney injury score (i.e., an indicator of kidney architectural damage), were substantially increased in IR animals. Of importance was that these parameters were reversed in IR animals after HBO or ADMSC therapy, and further reversed in IR animals after combined HBO-ADMSC treatment. Plentiful data have shown that angiogenesis plays a crucial role in restoring blood flow and improving ischemia-related/IR-related organ dysfunction [25-27]. A principal finding in the present study was that, as compared with IR animals, EPCs significantly increased both in circulation and in kidney parenchyma in IR animals treated by HBO-ADMSC. Additionally, angiogenesis factors markedly increased in IR animals treated by HBO-AMDSC compared to IR animals without treatment. These findings are comparable with those of previous studies [25-27], and can, at least in part, explain why podocyte components (i.e., the integrity of tubuloglomerular function) were significantly preserved in IR animals treated by HBO-ADMSC compared to IR only animals.

In conclusion, combined HBO-ADMSC therapy is innovative and effectively protected kidney from acute IR injury mainly by suppressing inflammation and oxidative stress and enhancing angiogenesis.

Acknowledgements

This study was supported by a program grant from Chang Gung Memorial Hospital, Chang Gung University (Grant number: CMRPG8G-0561).

Disclosure of conflict of interest

None.

Address correspondence to: Dr. Hon-Kan Yip, Division of Cardiology, Department of Internal Medicine, Kaohsiung Chang Gung Memorial Hospital and Chang Gung University College of Medicine, Kaohsiung 83301, Taiwan. Tel: +86-7-7317123 Ext. 8300; Fax: +86-7-7322402; E-mail: han.gung@msa.hinet.net

References

[1] Schrier RW, Wang W, Poole B and Mitra A. Acute renal failure: definitions, diagnosis, pathogenesis, and therapy. J Clin Invest 2004; 114: 5-14.

[2] Friedericksen DV, Van der Merwe L, Hattingh TL, Nel DG and Moosa MR. Acute renal failure in the medical ICU still predictive of high mortality. S Afr Med J 2009; 99: 873-875.

[3] Lameire N, Van Biesen W and Vanholder R. Acute renal failure. Lancet 2005; 365: 417-430.

[4] Parikh CR, Coca SG, Wang Y, Masoudi FA and Krumholz HM. Long-term prognosis of acute kidney injury after acute myocardial infarction. Arch Intern Med 2008; 168: 987-995.

[5] Pickering JW, James MT and Palmer SC. Acute kidney injury and prognosis after cardiopulmonary bypass: a meta-analysis of cohort studies. Am J Kidney Dis 2015; 65: 283-293.

[6] Romagnoli S, Ricci Z and Ronco C. CRRT for sepsis-induced acute kidney injury. Curr Opin Crit Care 2018; 24: 483-492.

[7] Thiele RH, Isbell JM and Rosner MH. AKI associated with cardiac surgery. Clin J Am Soc Nephrol 2015; 10: 500-514.

[8] Ali T, Khan I, Simpson W, Prescott G, Townend J, Smith W and Macleod A. Incidence and outcomes in acute kidney injury: a comprehensive population-based study. J Am Soc Nephrol 2007; 18: 1292-1298.

[9] Thadhani R, Pascual M and Bonventre JV. Acute renal failure. N Engl J Med 1996; 334: 1448-1460.

[10] Xue JL, Daniels F, Star RA, Kimmel PL, Eggers PW, Molitoris BA, Himmelfarb J and Collins AJ. Incidence and mortality of acute renal failure in Medicare beneficiaries, 1992 to 2001. J Am Soc Nephrol 2006; 17: 1135-1142.

[11] Chen YT, Tsai TH, Yang CC, Sun CK, Chang LT, Chen HH, Chang CL, Sung PH, Zhen YY, Leu S, Chang HW, Chen YL and Yip HK. Exendin-4 and sitagliptin protect kidney from ischemia-reperfusion injury through suppressing oxidative stress and inflammatory reaction. J Transl Med 2013; 11: 270.

[12] Chen YT, Yang CC, Zhen YY, Wallace CG, Yang JL, Sun CK, Tsai TH, Sheu JJ, Chua S, Chang CL, Cho CL, Leu S and Yip HK. Cyclosporine-assisted adipose-derived mesenchymal stem cell therapy to mitigate acute kidney ischemia-reperfusion injury. Stem Cell Res Ther 2013; 4: 62.

[13] Lin KC, Yip HK, Shao PL, Wu SC, Chen KH, Chen YT, Yang CC, Sun CK, Kao GS, Chen SY, Chai HT, Chang CL, Chen CH and Lee MS. Combination of adipose-derived mesenchymal stem cells (ADMSC) and ADMSC-derived exosomes for protecting kidney from acute ischemia-reperfusion injury. Int J Cardiol 2016; 216: 173-185.

[14] Yip HK, Yang CC, Chen KH, Huang TH, Chen YL, Zhen YY, Sung PH, Chiang HJ, Sheu JJ, Chang

CL, Chen CH, Chang HW and Chen YT. Combined melatonin and exendin-4 therapy preserves renal ultrastructural integrity after ischemia-reperfusion injury in the male rat. J Pineal Res 2015; 59: 434-447.
[15] Zhang R, Yin L, Zhang B, Shi H, Sun Y, Ji C, Chen J, Wu P, Zhang L, Xu W and Qian H. Resveratrol improves human umbilical cord-derived mesenchymal stem cells repair for cisplatin-induced acute kidney injury. Cell Death Dis 2018; 9: 965.
[16] Zhen YY, Yang CC, Hung CC, Lee CC, Lee CC, Wu CH, Chen YT, Chen WY, Chen KH, Yip HK and Ko SF. Extendin-4 protects kidney from acute ischemia-reperfusion injury through upregulation of NRF2 signaling. Am J Transl Res 2017; 9: 4756-4771.
[17] Sheffield PJ. How the Davis 2.36 ATA wound healing enhancement treatment table was established. Undersea Hyperb Med 2004; 31: 193-194.
[18] Slovut DP and Sullivan TM. Critical limb ischemia: medical and surgical management. Vasc Med 2008; 13: 281-291.
[19] Thom SR. Hyperbaric oxygen: its mechanisms and efficacy. Plast Reconstr Surg 2011; 127 Suppl 1: 131S-141S.
[20] Lin PY, Sung PH, Chung SY, Hsu SL, Chung WJ, Sheu JJ, Hsueh SK, Chen KH, Wu RW and Yip HK. Hyperbaric oxygen therapy enhanced circulating levels of endothelial progenitor cells and angiogenesis biomarkers, blood flow, in ischemic areas in patients with peripheral arterial occlusive disease. J Clin Med 2018; 7: 548.
[21] Yin TC, Wu RW, Sheu JJ, Sung PH, Chen KH, Chiang JY, Hsueh SK, Chung WJ, Lin PY, Hsu SL, Chen CC, Chen CY, Shao PL and Yip HK. Combined therapy with extracorporeal shock wave and adipose-derived mesenchymal stem cells remarkably improved acute ischemia-reperfusion injury of quadriceps muscle. Oxid Med Cell Longev 2018; 2018: 6012636.
[22] Chen KH, Chen CH, Wallace CG, Chen YT, Yang CC, Sung PH, Chiang HJ, Chen YL, Chua S, Yip HK and Cheng JT. Combined therapy with melatonin and exendin-4 effectively attenuated the deterioration of renal function in rat cardiorenal syndrome. Am J Transl Res 2017; 9: 214-229.
[23] Chen HH, Lin KC, Wallace CG, Chen YT, Yang CC, Leu S, Chen YC, Sun CK, Tsai TH, Chen YL, Chung SY, Chang CL and Yip HK. Additional benefit of combined therapy with melatonin and apoptotic adipose-derived mesenchymal stem cell against sepsis-induced kidney injury. J Pineal Res 2014; 57: 16-32.
[24] Sung PH, Sun CK, Ko SF, Chang LT, Sheu JJ, Lee FY, Wu CJ, Chua S and Yip HK. Impact of hyperglycemic control on left ventricular myocardium. A molecular and cellular basic study in a diabetic rat model. Int Heart J 2009; 50: 191-206.
[25] Chen YL, Tsai TH, Wallace CG, Chen YL, Huang TH, Sung PH, Yuen CM, Sun CK, Lin KC, Chai HT, Sheu JJ, Lee FY and Yip HK. Intra-carotid arterial administration of autologous peripheral blood-derived endothelial progenitor cells improves acute ischemic stroke neurological outcomes in rats. Int J Cardiol 2015; 201: 668-683.
[26] Huang TH, Chen YT, Sung PH, Chiang HJ, Chen YL, Chai HT, Chung SY, Tsai TH, Yang CC, Chen CH, Chen YL, Chang HW, Sun CK and Yip HK. Peripheral blood-derived endothelial progenitor cell therapy prevented deterioration of chronic kidney disease in rats. Am J Transl Res 2015; 7: 804-824.
[27] Lee FY, Chen YL, Sung PH, Ma MC, Pei SN, Wu CJ, Yang CH, Fu M, Ko SF, Leu S and Yip HK. Intracoronary transfusion of circulation-derived CD34+ cells improves left ventricular function in patients with end-stage diffuse coronary artery disease unsuitable for coronary intervention. Crit Care Med 2015; 43: 2117-2132.

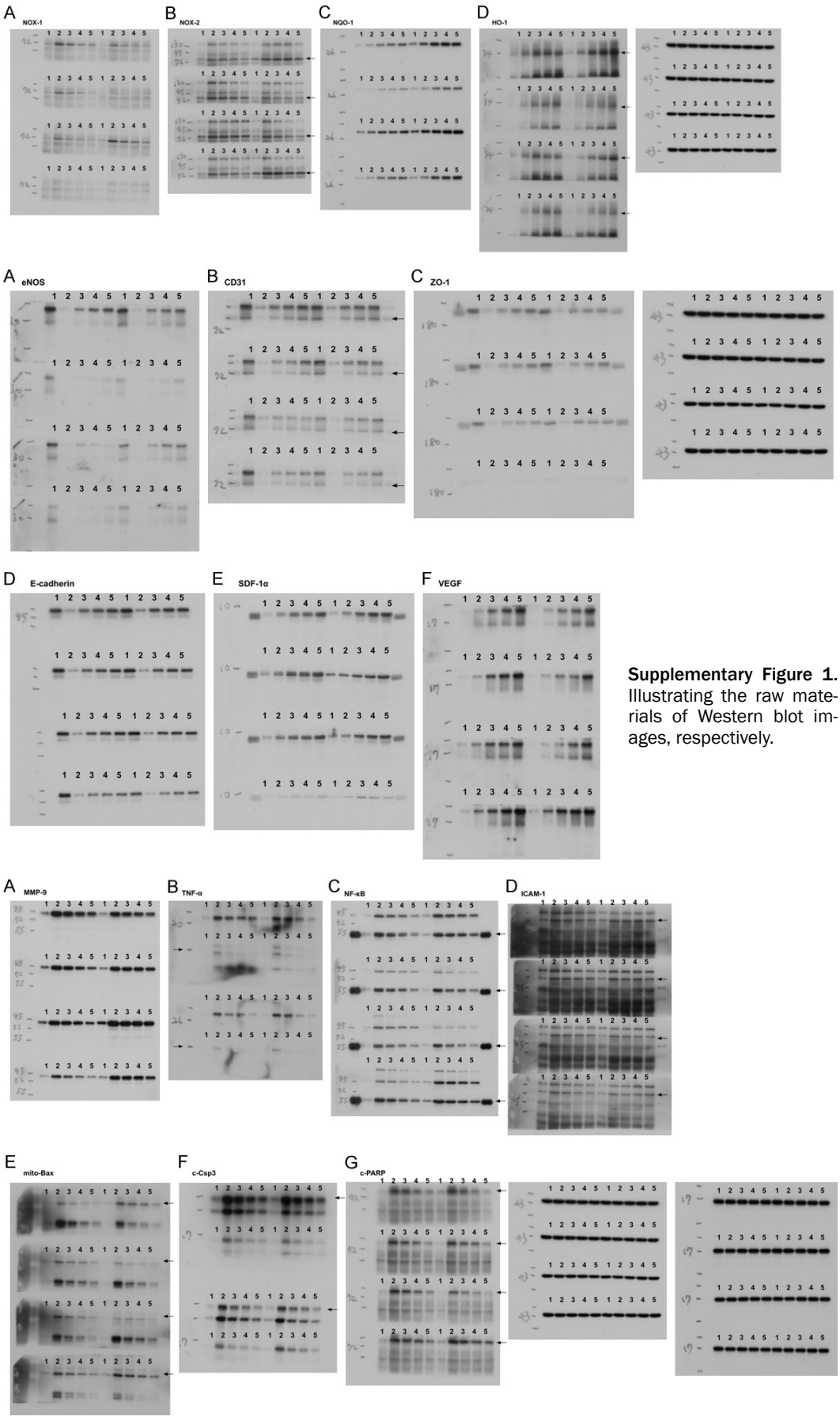

Supplementary Figure 1. Illustrating the raw materials of Western blot images, respectively.